

Disentangling the Kinematics and Stellar Populations of Counter-rotating Stellar Discs in Galaxies

Lodovico Coccato¹Lorenzo Morelli^{2, 3}Alessandro Pizzella^{2, 3}Enrico Maria Corsini^{2, 3}Lucio Maria Buson³Elena Dalla Bontà^{2, 3}¹ ESO² Dipartimento di Fisica e Astronomia
“G. Galilei”, Università degli Studi di
Padova, Italy³ INAF–Osservatorio Astronomico di
Padova, Italy

Spectroscopic VIMOS/IFU observations are presented for three galaxies known to host two stellar counter-rotating discs of comparable sizes. For the first time both the kinematics and stellar population properties of the two counter-rotating discs in the observed galaxies were separated and measured. The secondary, less massive, stellar component rotates in the same direction as the ionised gas and is on average younger and less metal-rich than the main galaxy disc. These results support the scenario of gas accretion followed by star formation as the origin for large counter-rotating stellar discs in galaxies, and set an upper limit of 44% to those formed by binary galaxy mergers.

Counter-rotating galaxies

Counter-rotating galaxies are those that host two components that rotate in opposite directions to each other. These peculiar objects have been observed in all morphological types, from ellipticals to spirals. They are classed by the nature (stars vs. stars, stars vs. gas, gas vs. gas) and size (counter-rotating cores, rings, discs) of the counter-rotating components (see Bertola & Corsini [1999] for a review). In this work, we investigate the peculiar class of counter-rotating galaxies with two counter-rotating stellar discs of comparable size. The prototype of this class of objects is the famous E7/S0 galaxy NGC 4550, whose counter-rotating nature was first discovered by Rubin et al. (1992). To date, there are only a few known counter-rotating galaxies similar to NGC 4550, but the census will increase as a result of the new two-dimensional spectroscopic surveys.

Different scenarios have been proposed to explain the formation of these peculiar objects. The internal origin scenario (Evans & Collett, 1994) describes the dissolution of a triaxial potential or a bar. In this process, the stars, moving on box orbits, escape from the confining azimuthal potential well and move onto tube orbits. During this process, half of the box-orbit stars are scattered onto clockwise-streaming tube orbits, the other half onto counterclockwise ones. In this way, two identical counter-rotating stellar discs can be built. In the gas accretion scenario, a disc galaxy acquires gas from extragalactic reservoirs onto retrograde orbits (e.g., Pizzella et al., 2004). If the amount of acquired gas is sufficiently large, the new gas drives away the pre-existing gas and it settles onto a counter-rotating disc. New stars are then born from the acquired gas, forming the counter-rotating stellar disc. In the binary merger scenario (e.g., Crocker et al., 2009), two disc galaxies with opposite spin directions collide and form two coplanar counter-rotating stellar discs, depending on the geometry of the encounter.

These different formation mechanisms are expected to leave differing signatures in the properties of the stellar populations of the counter-rotating component. In particular, age is a key element in differentiating among these scenarios. The internal origin predicts the same mass, luminosity, chemical composition and age for both counter-rotating stellar components. Gas acquisition followed by star formation predicts younger ages for the counter-rotating stellar component in all cases, and it allows for different metallicity and α -enhancement between the two discs. Direct acquisition of stars through mergers also allows for different metallicity and α -enhancement, but the younger component will be determined by the difference in age between the host galaxy and the merged system. Roughly, one would expect younger counter-rotating stars in ~ 50% of the cases.

A proper spectroscopic decomposition that separates the relative contribution of the two counter-rotating stellar components to the observed galaxy spectrum is therefore needed. In this way, the kinematics and the stellar populations of both the stellar components can be measured

simultaneously, allowing the different formation scenarios to be disentangled.

Results of the spectroscopic observations

We started an observational campaign with the integral field unit (IFU) of the VIMOS spectrograph at the VLT aimed at determining the most efficient mechanisms in building large-scale counter-rotating stellar discs, like those observed in NGC 4550. For this study, we developed a new spectroscopic decomposition technique that fits a galaxy spectrum and separates the contributions of two counter-rotating stellar components (Coccato et al., 2011). At each position on the sky, the code builds two synthetic templates (one for each stellar component) as a linear combination of spectra from an input stellar library, and convolves them with two Gaussian line-of-sight velocity distributions with different kinematics. Gaussian functions are also added to the convolved synthetic templates to account for ionised gas emission lines ($H\gamma$, $H\beta$, $[O III]$ and $[N I]$).

The spectroscopic decomposition code returns the spectra of two best-fit synthetic stellar templates and ionised gas emission (Figure 1), along with the best-fitting parameters of luminosity fraction, velocity and velocity dispersion. The line strengths of the Lick indices of the two counter-rotating components are measured on the two best-fit synthetic templates. We then compare the indices $H\beta$, Mgb , $Fe5270$, and $Fe5335$ to the predictions of stellar population models to infer the stellar age, metallicity ($[Z/H]$), and abundance ratio of α -elements ($[\alpha/Fe]$) of the two counter-rotating discs. We also computed the mass-to-light ratios and the mass fraction of the two counter-rotating components from the luminosity fraction and the inferred stellar population parameters. The estimated mass is used to determine which component is the main (i.e., the most massive) and which is the secondary (i.e., the least massive).

We started this project (programme IDs: 383.B-0632 and 087.B-0853A) by observing with VIMOS/IFU three galaxies that were known to host counter-rotating stellar discs of comparable size: NGC 3593 (Bertola et al., 1996), NGC 4550 (Rubin et al., 1992) and NGC 5719 (Vergani et al.,

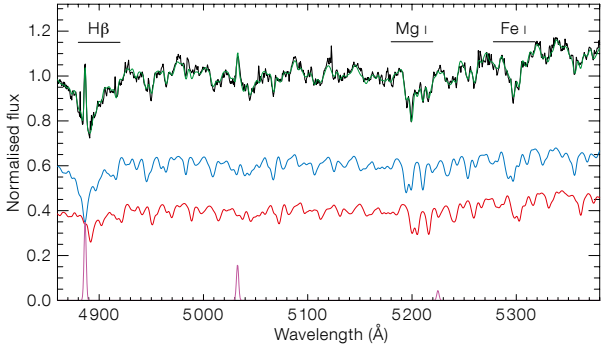


Figure 1. Fit of the galaxy spectrum (black) in a spatial bin. The best-fitting model (green) is the sum of the spectra of the ionised gas component (magenta) and the two stellar components (blue and red). The differences in the position of absorption line features and in the H β equivalent widths between the two stellar components (indicating different kinematics and stellar population content) are clearly evident.

Table 1. Luminosity-weighted values for the stellar population parameters of the stellar discs.

	Age [Gyr]	[Z/H]	[α /Fe]
NGC 3593			
Main:	3.6 ± 0.6	-0.04 ± 0.03	0.09 ± 0.02
Secondary:	2.0 ± 0.5	-0.15 ± 0.07	0.18 ± 0.03
NGC 4550			
Main:	6.9 ± 0.6	-0.01 ± 0.03	0.20 ± 0.02
Secondary:	6.5 ± 0.5	-0.13 ± 0.04	0.28 ± 0.02
NGC 5719			
Main:	4.0 ± 0.9	0.08 ± 0.02	0.10 ± 0.02
Secondary:	1.3 ± 0.2	0.3 ± 0.02	0.14 ± 0.02

2007). The combination of the collecting power of an 8-metre-class telescope, the large wavelength coverage (4150–6200 Å) and the high spectral resolution (full width half maximum [FWHM] of 2.0 Å) with the HR-blue grism makes VIMOS on the VLT the best-suited integral field unit for this kind of study.

In all the sample galaxies, we confirm the presence of two stellar discs of comparable size, and one ionised gas component. The secondary stellar component and the ionised gas component counter-rotate with respect to the main stellar disc. Moreover, in all the observed galaxies, these counter-rotating secondary components

are younger, more metal-poor, and have higher abundances of α -elements than the main stellar discs.

Table 1 summarises the mean properties of the two counter-rotating stellar populations, and Figures 2, 3 and 4 illustrate our results. In these figures, the extension of the VIMOS/IFU field of view is plotted over the galaxy image (upper-left panels). The collected spectra are then spatially binned over the field of view with the Voronoi binning technique to increase the signal-to-noise ratio (see Coccato et al. [2013] for further details). The spectral decomposition technique is then applied on the spectrum of each spatial bin to measure

the kinematics and the Lick indices of the fitted components. The measured kinematics are used to construct the two-dimensional velocity fields, where the structure of the adopted spatial binning is still visible, and the counter-rotation between the two stellar components is remarkable (lower panels). The Lick indices are shown in the diagnostic plots (upper right panels) with the predictions of single stellar population models (Thomas et al., 2011). We use H β and the combined $[\text{MgFe}]' = \sqrt{(\text{Mgb} \cdot 0.82 \cdot \text{Fe5270} + 0.28 \cdot \text{Fe5335})}$ index as indicator of stellar age and metallicity. We also take into account the variation in the abundance of α -elements and metallicity by measuring

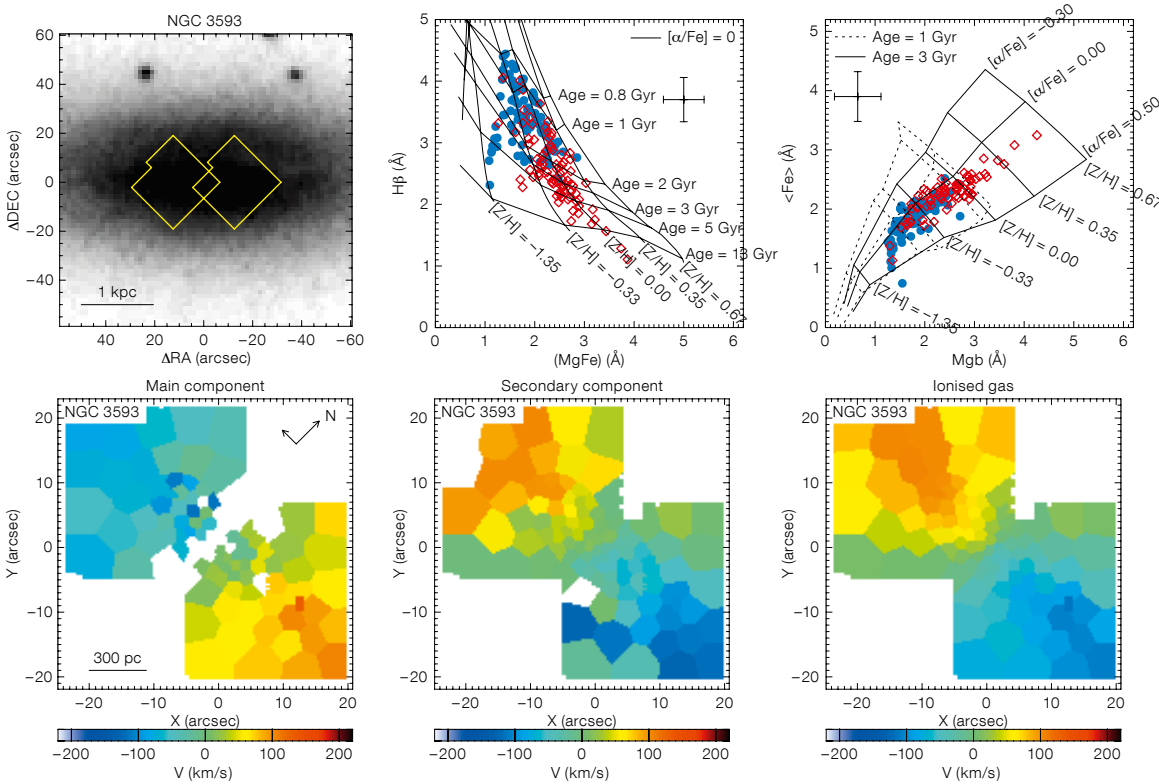


Figure 2. Results of the spectroscopic decomposition of NGC 3593. The top left panel shows the galaxy image with the location of the VIMOS observed field of view. The bottom panels show the two-dimensional kinematics of the main, secondary and ionised gas components, respectively. The top-right panels show the measured equivalent width of the Lick indices; grids with the predictions from single stellar population models are also shown. The crosses on the top-right side of the panels show the mean error bars on the measured indices. Each spatial bin returns two sets of Lick indices, one for each stellar component: red symbols represent the main stellar component, whereas blue symbols represent the secondary counter-rotating component.

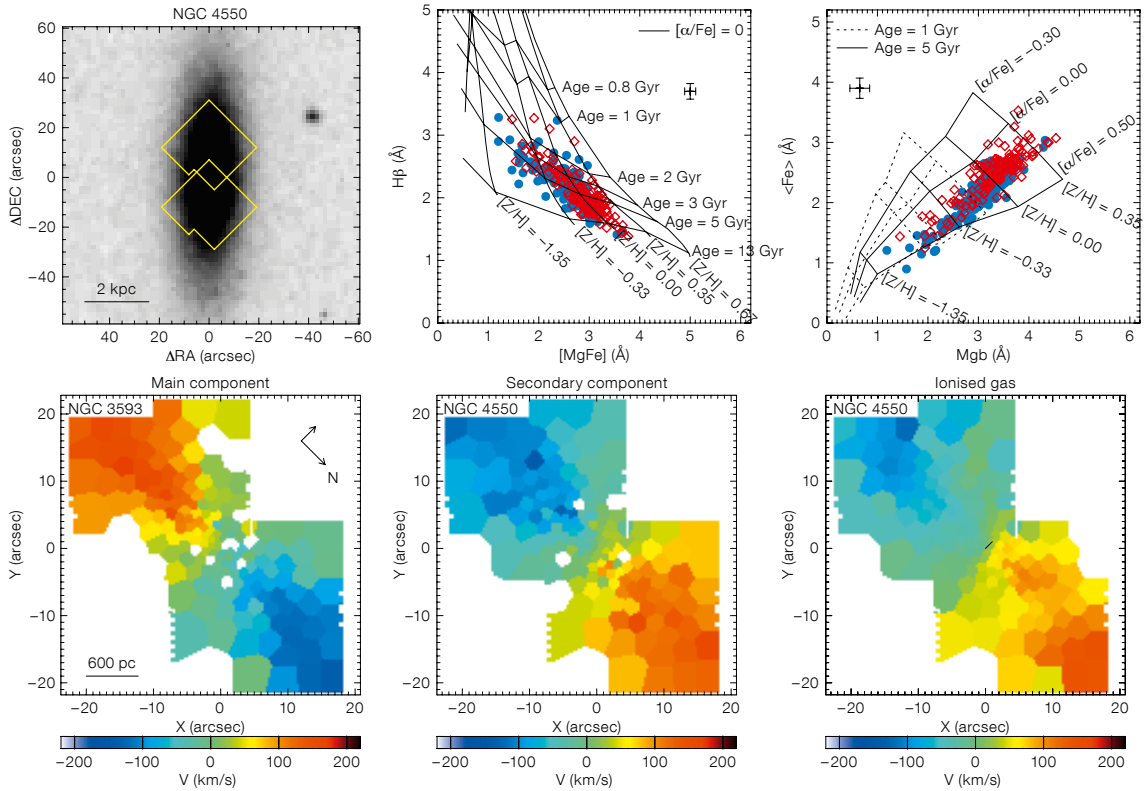


Figure 3. As Figure 2, but for NGC 4550.

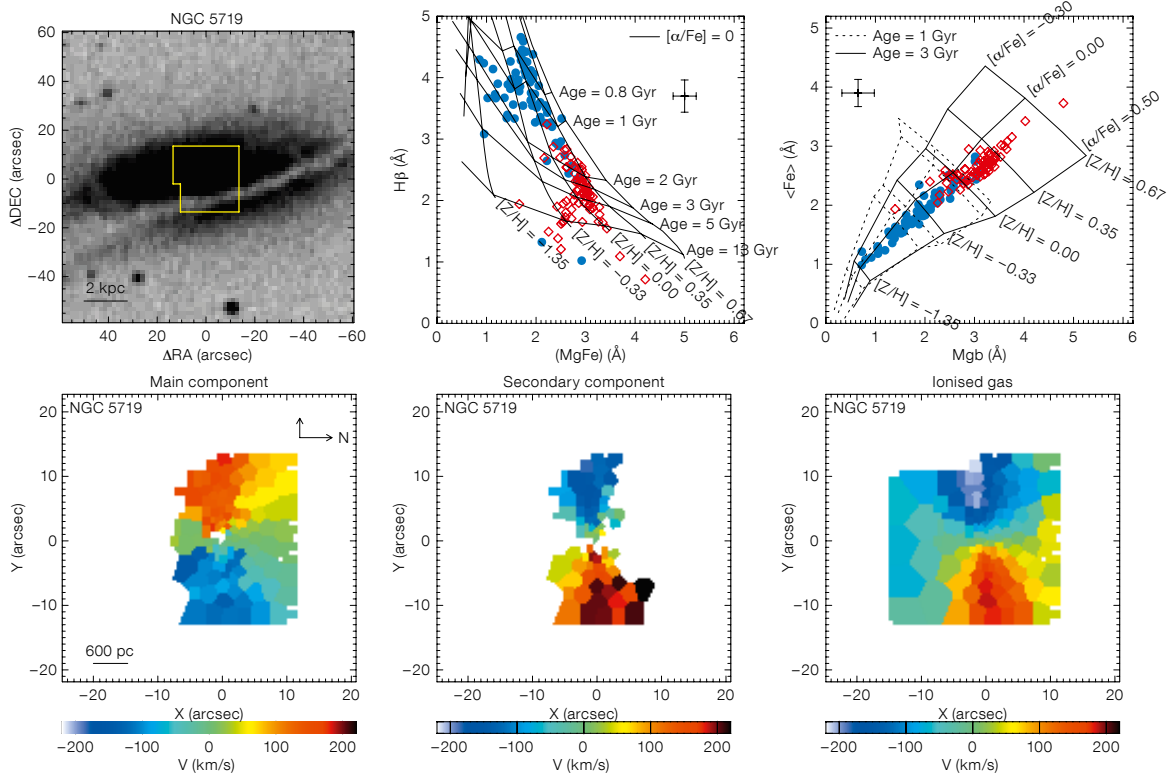


Figure 4. As Figure 2, but for NGC 5719.

the magnesium Mgb index and the mean iron index $\langle \text{Fe} \rangle = (\text{Fe}5270 + \text{Fe}5335)/2$.

NGC 3593. An isolated, highly inclined, S0/a spiral at a distance of 7 Mpc. It is characterised by a patchy spiral dust pattern in the centre. The two counter-rotating stellar discs have different scale lengths, but the same intrinsic flattening. The secondary component dominates the innermost 500 pc. The ages of the two components date the accretion event to between 2.0 and 3.6 Gyr ago, i.e., 1.6 ± 0.8 Gyr after the formation of the main stellar disc (Coccato et al., 2013).

NGC 4550. An E7/S0 galaxy in the Virgo Cluster, at a distance of 16 Mpc, and it is often indicated as the prototype of galaxies with counter-rotating stellar discs. It has an elliptical galaxy nearby, NGC 4551, to the northeast of NGC 4550 at a projected distance of 14 kpc. An interaction in the past between these two systems could have produced the counter-rotating stellar disc in NGC 4550, although no photometric signatures of the interaction, such as tidal tails or gas streams, have been detected. The two counter-rotating stellar discs in NGC 4550 have the same scale lengths, but slightly different ellipticity ($\epsilon_{\text{main}} = 0.6$, $\epsilon_{\text{second}} = 0.5$) meaning that they have different scale heights. The measured ages date the accretion event ~ 7 Gyr ago, i.e. less than 1 Gyr after the formation of the main stellar disc (Coccato et al., 2013).

NGC 5719. An Sab galaxy at a distance of 23 Mpc, and a member of a rich group. It is currently interacting with the Sbc galaxy NGC 5713, which is to the west of NGC 5719 at a projected distance of 77 kpc. The interaction between the two systems is traced by a bridge of neutral hydrogen (Vergani et al., 2007), which fuels the secondary counter-rotating stellar component in NGC 5719. The two stellar components in NGC 5719 have similar luminosity, but the secondary is less massive because of its younger age. Moreover, the youngest ages are observed in the secondary component at ~ 700 pc from the centre, where the H β emission lines are more intense (Coccato et al., 2011). The ages of the two components date the accretion event between 1.3 and 4.0 Gyr ago, i.e. 2.7 ± 0.9 Gyr after the formation of the main stellar disc (Coccato et al., 2011).

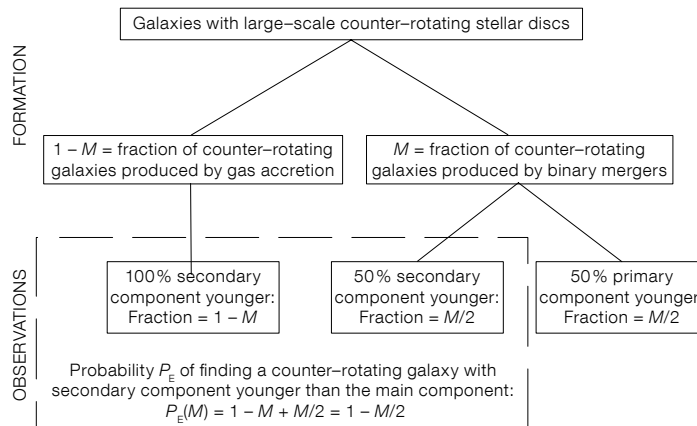


Figure 5. Schematic representation of the probability P_E of observing the secondary stellar disc younger than the main galaxy disc, as a function of the fraction M of galaxies formed through the binary galaxy merger scenario.

The most efficient mechanism to build counter-rotating stellar discs

Our results favour the external origin of the counter-rotating components in all the three observed galaxies, and discard the internal origin scenario. As stated above, in the gas-accretion scenario the stellar component associated with the ionised gas is predicted to always be younger than the main stellar component. In binary galaxy mergers instead, one would expect that the younger stellar component is associated with the ionised gas only in 50% of the cases. Although we always observe the secondary component to be younger than the main galaxy disc, thus favouring the gas accretion scenario, we cannot rule out the binary galaxy merger scenario.

On the other hand, we can infer an upper limit to the fraction of galaxies with two counter-rotating stellar discs that were formed by binary mergers by statistical arguments. We define M as the fraction of galaxies hosting two counter-rotating stellar discs of comparable sizes that were generated by a binary major merger (thus, $(1 - M)$ is the fraction produced by gas accretion), and E as the event of finding the stellar component co-rotating with the gas to be the youngest. The probability P_E to observe E is: $P_E = 1 - M/2$ (see Figure 5). The probability $\Pi_E(M)$ of observing E in exactly N galaxies out of a sample of T counter-rotating galaxies is given by the first term of the binomial distribution. It is therefore possible to compute the most probable value for the fraction of counter-rotating galaxies produced by binary mergers, M_{MAX} , simply by maxi-

mising $\Pi_E(M)$. In our case $N = T = 3$, therefore $M_{\text{MAX}} < 44\%$ at 1σ confidence level.

Thus, it is fundamental to measure the difference in ages of the counter-rotating components in a larger sample of counter-rotating galaxies to identify the most efficient mechanism and derive more precise constraints. Large spectroscopic surveys like MaNGA will help to identify other potential candidates by recognising the kinematic signatures of stellar counter-rotating discs, such as the two symmetric peaks in the velocity dispersion map. The MaNGA survey is one of the Next Generation Sloan Digital Sky Surveys, and it will collect IFU spectroscopic data for $\sim 10\,000$ galaxies in the nearby Universe within six years. Moreover, the next generation integral field unit MUSE at the VLT will represent a significant step forward for these studies, because of the better spectral resolution, wavelength coverage and field of view with respect to VIMOS.

References

- Bertola, F. & Corsini, E. M. 1999, IAU Symposium, 186, *Galaxy Interactions at Low and High Redshift*, eds. Barnes, J. E. & Sanders, D. B. (Dordrecht: Kluwer), 149
- Bertola, F. et al. 1996, ApJ, 458, L67
- Coccato, L. et al. 2011, MNRAS, 412, L113
- Coccato, L. et al. 2013, A&A, 549, 3
- Crocker, A. F. et al. 2009, MNRAS, 393, 1255
- Evans, N. W. & Collett, J. L. 1994, ApJ, 420, L67
- Pizzella, A. et al. 2004, A&A, 424, 447
- Rubin, V. C., Graham, J. A. & Kenney, J. D. P. 1992, ApJ, 394, L9
- Thomas, D., Maraston, C. & Johansson, J. 2011, MNRAS, 412, 2183
- Vergani, D. et al. 2007, A&A, 463, 883